Structural Engineering and Mechanics, *Vol. 67, No. 4 (2018) 347-358*
DOI: https://doi.org/10.12989/sem.2018.67.4.347

Shear strength of non-prismatic steel fiber reinforced concrete beams without stirrups

Musab Aied Qissab*[1] and Mohammed Munqith Salman[2a]

[1]*Department of Civil Engineering, Al-Nahrain University, Baghdad, Iraq*
[2]*Department of Civil Engineering, Dijlah University College, Baghdad, Iraq*

(Received March 15, 2018, Revised June 3, 2018, Accepted June 10, 2018)

Abstract. The main aim of this research was to investigate the shear strength of non-prismatic steel fiber reinforced concrete beams under monotonic loading considering different parameters. Experimental program included tests on fifteen non-prismatic reinforced concrete beams divided into three groups. For the first and the second groups, different parameters were taken into consideration which are: steel fibers content, shear span to minimum depth ratio (a/d_{min}) and tapering angle (α). The third group was designed mainly to optimize the geometry of the non-prismatic concrete beams with the same concrete volume while the steel fiber ratio and the shear span were left constant in this group. The presence of steel fibers in concrete led to an increase in the load-carrying capacity in a range of 10.25%-103%. Also, the energy absorption capacity was increased due to the addition of steel fibers in a range of 18.17%-993.18% and the failure mode was changed from brittle to ductile. Tapering angle had a clear effect on the shear strength of test specimens. The increase in tapering angle from (7°) to (12°) caused an increase in the ultimate shear capacity for the test specimens. The maximum increase in ultimate load was 45.49%. The addition of steel fibers had a significant impact on the post-cracking behavior of the test specimens. Empirical equation for shear strength prediction at cracking limit state was proposed. The predicted cracking shear strength was in good agreement with the experimental findings.

Keywords: shear strength; non-prismatic beams; steel fiber; tapering angle; reinforced concrete

1. Introduction

Non-prismatic reinforced concrete beams or varied-depth concrete beams have been used in buildings in the last decades. These beams are often used in various structures such as beam in mid-rise buildings, metro train pier cap (Fig. 1) and continuous bridges for aesthetic and economic reasons. These types of structural members are supposed not only to be more economic, but also to resist load better than that of the prismatic beam. However, there is still little information about experimental data for predicting the shear behavior of non-prismatic reinforced concrete beams (Tena-Colunga *et al*. 2002, Hai *et al*. 2009). The addition of fibers to the brittle material such as concrete can offer a suitable practical and economical method of overcoming the weakness in tensile strength and improves many of the structural properties such as flexural strength, thermal shock, resistance to fatigue impact, and enhances the ductility of the material (Mahadik *et al*. 2014, Riza 2017). The enhanced properties of fibers include compressive strength, tensile strength, elastic modulus, crack control, crack resistance, fatigue life, durability, resistance to impact and abrasion, thermal characteristics, shrinkage, expansion, and fire resistance. Numerous researches, experimentation, development, and industrial application of steel fiber reinforced concrete have been carried out (James *et al*. 2002).

Fig. 1 Pier cap of Delhi metro train project

Alejandro *et al*. (2012) studied the effect of load distribution and variable depth on shear resistance of slender beams without stirrups. The experimental program consists of eight slender beams without stirrups. Four specimens had a constant depth, whereas the others had variable depths (maximum depth of 600 mm). Each specimen was tested twice: one side was tested first under point loading, and then (after repairing) the other side was tested under either uniform loading or triangular loading.The investigated parameters were: influence of load distribution (point loading, uniform loading, and triangular loading) and influence of variable depth. The experimental

∗Corresponding author, Assistant Professor
E-mail: musabaq79@gmail.com
[a]Assistant Lecturer
E-mail: mohammed.munqith7@gmail.com

http://www.techno-press.com/journals/sem&subpage=7
ISSN: 1225-4568 (Print), 1598-6217 (Online)

results showed a significant influence of the type of loading and of tapered geometries on the shear strength. For the constant-depth cantilevers tested, the same elements carried 27% more load for uniformly distributed loading than for point loading, and more than 100% for triangular loading than for point loading.In the case of variable depth, the increase in the load was 63% more than 100% for distributed loading and triangular loading respectively.

Chenwei *et al*. (2015) studied the shear resistance of reinforced concrete haunch beam without stirrup. Experiments were conducted on three reinforced concrete haunched beams with different haunch positions. The inclination of the bottom surface and tensile bars (α) was fixed at (11.3°). It was found from the test results that the haunched shape of reinforced concrete haunch beam resulted in arch action even in the slender beam, but the arch action contributions varied in accordance with variations in the cracking pattern.

Vu Hong (2011) investigated the shear resistance of haunched concrete beams without shear reinforcement. The experimental program included tests on 18 specimens. All test specimens were designed to have the same geometry for a bridge deck's slab in practice. The results observed from the experimental program and nonlinear FEM analysis showed that the region of failure of haunched beams was close to the support (minimum depth). At failure load, the critical shear crack seemed to be a moreover development of a formerly pure shear crack in the disturbed stress region near the support. The lower end of this shear crack tends downward to the position of the longitudinal reinforcements while the top end passes through the concrete compression zone. The failure occurred after the critical crack penetrates the compression zone. Therefore, a critical state was assumed at which the critical shear crack has already occurred, but it does not break through the compression zone yet.

Sasturkar (2012) studied the performance and serviceability of fiber reinforced concrete beams. The investigation consisted of tests on ten full-size reinforced concrete tapered beams. The test specimens had 2000 mm overall span and a width of 150 mm. At mid-span of the beam, the depth was kept constant and equal to 285 mm. The test specimens were divided into two series, the first series consisted of five specimens without steel fiber whereas the remaining contained steel fibers as additional reinforcement up to 3/4 of the specimen from the bottom and spread uniformly in the specimen. The values of the inclination angle used were (2, 4, 6, 8 and 10) degrees. The volume fraction of fibers used in this study was kept constant and equal to 1.15%. The results obtained from the experimental investigation showed an increase in the load of 10%, 12%, and 42% was observed in specimens having a tapering angle of 2, 6 and 10 degrees respectively. A reduction of 10% in load was observed when the tapered angle was 4°. It was noticed that the ultimate load carrying capacity of beams with steel fiber was increased by 6%, 30%, 20% and 25% for beams with a tapering angle of 2, 4, 8 and 10 degrees respectively, while the load remained constant for the beam with a tapering angle of 6 degrees.

Daniel *et al*. (2014) studied the behavior of shear strength of steel fiber-reinforced concrete beams. The experimental program consisted of six reinforced concrete beams with and without steel fibers. Prisms were tested under four-point bending to evaluate steel fiber contribution to the shear strength. Straight, hook-end steel fibers were used in this study, which had a length of 35 mm and aspect ratio of 65. It was found from the results that the steel fibers had a greater contribution to shear strength of reinforced concrete beams and reduce the crack width, which in turn leads to a possible reduce in a number of stirrups in a concrete beam. Empirical equations were used to evaluate beam capacity and it was found that a high variability obtained from these equations, while some of these equations had not properly predicted the ultimate shear strength of the steel fiber-reinforced concrete beams.

Babar *et al*. (2015) studied the shear strength of steel fiber reinforced concrete beams without stirrups. Experiments were conducted on fifteen deep beams. The shear span to depth ratio (*a/d*) was 1, 1.25 and 1.5, and all beams were rectangular in cross section with 125 mm width. M-25 grade concrete was used for tested specimens. The results obtained from experimental investigation indicated that the addition of steel fibers decreases the width and size of crack and increases the deformation capacity. The maximum increase in ultimate shear stress was about 60.7% for shear span to depth ratio of 1.0 and fiber content of 2.0%, also, the maximum increase in cracking shear stress value was 54.54% compared to normally reinforce concrete beam which was obtained for shear span to depth ratio of about 1.0 and steel fiber content of about 2.0 %.

ASCE- ACI Task Committee 426 (1973) showed that there are various modes of failure with respect to shear span to depth ratio (*a/d*). First, true shear failure, this failure happens in deep beams, which have a shear span to depth ratio ($0<a/d<1$). Second, shear tension or shear compression failure, occur in short beams with shear span to depth ratio ($1<a/d<2.5$). Third, diagonal tension failure, for normal and long beams of rectangular cross section with shear span to depth ratio ($a/d>2.5$). For reinforced concrete beams with shear span to depth ratio (*a/d*) greater than 6, flexural failure is governed.

Mohammed (2014) (proposed a method that combines both statistical regression analysis and dimensional analysis for predicting the shear capacity of slender reinforced concrete beams without stirrup. In which the size effect was taking into consideration. The method was combined with the modified Buckingham-PI theorem to form two mathematical models for predicting the ultimate shear strength and the shear capacity of diagonal tension cracks. The results obtained showed that the experimental ultimate shear strength reduced drastically as the (*a/d*) value increases from 1 to 2.5 and the shear strength decreased much more slowly.

Sudheer *et al*. (2010) investigated the shear resistance of high strength concrete HSC beams without stirrup with different shear span-depth ratios (a/d=1, 2, 3 and 4) and compared the test results with the shear models and available database to predict the shear strength of reinforced concrete beams. It was found from the experimental results

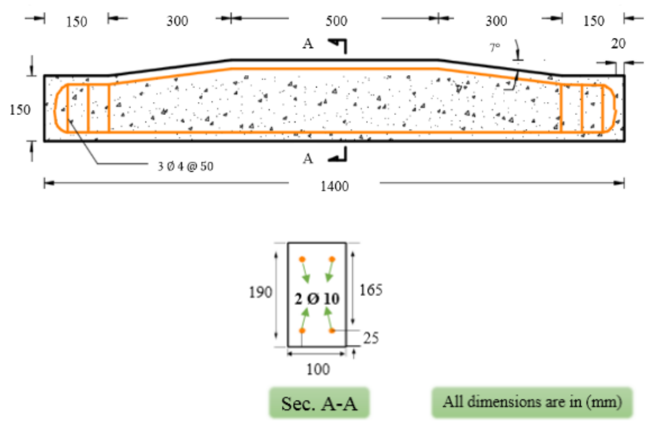

Fig. 2 Details of test specimens for group *G*1

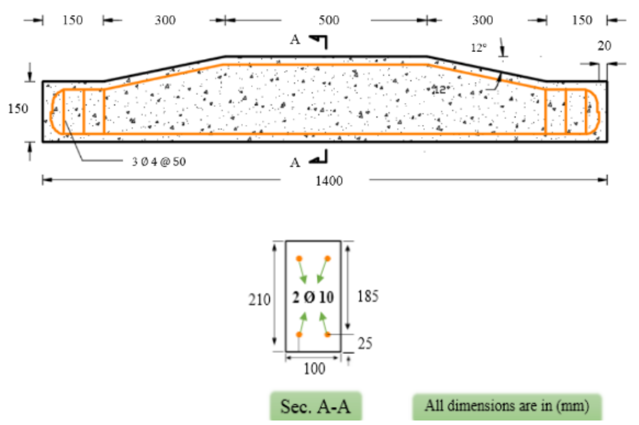

Fig. 3 Details of test specimens for group *G*2

that the shear span-depth ratio (*a/d*) had significant effect on the shear capacity of concrete beams, the strut action prevails when the shear span-depth ratio (*a/d*) was less than 2.0, and the shear resistance was very high, while the shear strength showed remarkable increase in shear span-depth ratios (*a/d*) up to 2 in compared with the various design approaches.The scope of the present investigation is to study the shear behavior of non-prismatic reinforced concrete beams without shear reinforcement. The parameters considered in this study were: fiber volume fraction (*Vf*), tapered angle (α) and shear span to depth ratio (*a/d*). The mechanical properties of steel fiber reinforced concrete were also investigated.

2. Experimental investigation

2.1 Test specimens

The experimental program comprised tests on fifteen test specimens which are divided into three groups: group (*G*1), group (*G*2), and group (*G*3). There were six simply supported non-prismatic reinforced concrete beams for groups (*G*1) and (*G*2) while group (*G*3) contained three test specimens. The details of test specimens for groups (*G*1), (*G*2), and (*G*3) are shown in Figs 2, 3, and 4 respectively. All test specimens in the group (*G*3) had the same concrete volume and steel fiber content but they have different geometry. The properties of the tested specimens and their details are presented in Table 1. Fig. 5 shows the reinforcement details and test specimen ready for testing.

2.2 Materials

The type of cement used was ordinary Portland cement Type (I). Natural sand passing through (4.75) mm sieves and a local naturally crushed aggregate of maximum size

Table 1 Properties of tested specimens for groups *G*1, *G*2, and *G*3

Group	Specimen Designation	Geometry	S.F% by vol. of concrete	Tapered angle (α)	a/d_{min}
	G1B1		0		1.6
	G1B2		0.5		1.6
*G*1	G1B3		0.75		1.6
	G1B4		0	7°	2.8
	G1B5		0.5		2.8
	G1B6		0.75		2.8
	G2B1		0		1.6
	G2B2		0.5		1.6
*G*2	G2B3		0.75		1.6
	G2B4		0	12°	2.8
	G2B5		0.5		2.8
	G2B6		0.75		2.8
	G3B1		0.5	0°	2.4
*G*3	G3B2		0.5	15°	3.36
	G3B3		0.5	15°	3.36

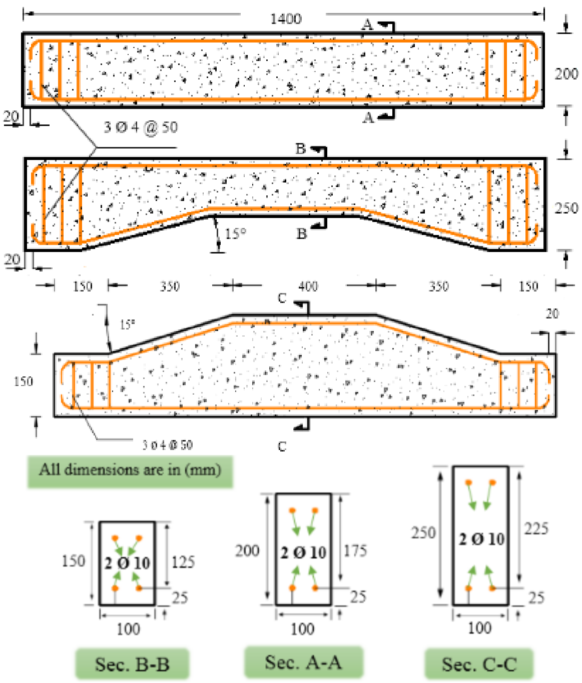

Fig. 4 Details of test specimens for group *G*3

Fig. 5(a) Reinforcement details

Fig. 5(b) Test specimens ready for testing

(12.5) mm were used. Ordinary tap water was used in the experimental work for mixing and curing concrete. The quantity of materials for concrete mixtures are given in Table 2. Zinc galvanized with silver color steel fibers were used in this study which have a cylindrical geometry with an aspect ratio (62.5) and average length of (50) mm with hooked ends (Sika ViscoCrete -5930).

Table 2 Concrete mixture proportions for reference specimens

Mixture type	Quantity of material					
	Cement kg/m^3	Sand (kg/m^3)	Gravel (kg/m^3)	Water (lit/m^3)	S.P.% by wt. of cement	W/C
Reference mixture	420	850	1030	181	0.35	0.43
Mixture with (0.5%) steel fibers	420	850	1030	181	0.55	0.43
Mixture with (0.7%) steel fibers	420	850	1030	181	0.7	0.43

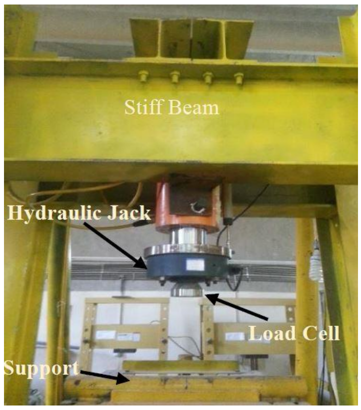

Fig. 6 Test instrumentation

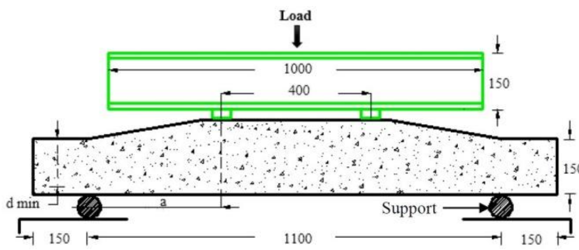

Fig. 7 Schematic diagram of the test setup

2.3 Instrumentation and test procedure

Each specimen was fixed in a testing machine with a hydraulic jack of 1000 kN capacity. The specimen supported by two rollers and loaded monotonically up to failure. Fig. 6 shows the testing instruments. A steel beam (I-section) with a total span of 1000 mm was used to distribute the applied load from the load cell into two point load by two steel plates having dimensions of 50 mm width and 150 mm for length. After each loading step, the loading was stopped for about 3 minutes so any crack formation on the two faces of each test specimen can be highlighted. The load of the first shear crack and the corresponding displacement at the loading points and also the ultimate loads were recorded. The beam deflection at the loading points was recorded automatically by the loading piston which is a characteristic of the loading system used. Fig. 7 describes the test setup of the test specimens.

3. Results and discussion

3.1 Compressive strength

The test was carried out on cubes of size (150×150×150) mm according to BS 1881: part 116:1989. The specimens were tested using compression testing machine type (ELE) with a capacity of 2000 kN and a rate of loading equal to 0.3 MPa/sec. The average compressive strength of three cubes at age of 28 days was recorded. According to the test results, the compressive strength of concrete slightly increases with the increase of steel fiber percentage. This is because steel fibers transmit the load in every direction, perfectly holds the micro-cracks in the concrete structure, and reduce crack width that leads to increasing the concrete cracking resistance during the loading process. However, the function of steel fibers was activated obviously in the tensile strength test.

3.2 Splitting tensile strength

The test was carried out on cylindrical specimens of dimensions 150 mm diameter and 300 mm length in accordance with the ASTM C496/C496M-05. The test was implemented using compression testing machine with a capacity of 2000 kN and a rate of loading of 0.028 MPa/sec. For each mixture, three cylinders were tested and their average value was adopted. According to the test results, the splitting tensile strength increases with the increase of steel fibers percentage. The maximum increase in tensile strength was obtained from the cylinder with steel fiber of 0.75% by volume of concrete. The reason behind this related to the resistance of crack propagation by steel fibers which enhance the concrete cracking resistance and tensile strength during loading.

3.3 Flexural strength

Tests were carried out on prisms with dimensions of (100×100×400) mm under two point monotonic loading according to ASTM C-78, 2002. The test was carried out using the flexural machine for plain concrete and prism type (MATEST) with a capacity of 150 kN. It has been observed from the given results, that the modulus of rupture increases with the increase of steel fibers ratio. This enhancement is mainly due to the interlocking action of fibers, and that the steel fibers improve the ductility of concrete. A random distribution and orientation of steel fibers provide reinforcement for the small weak regions in three dimensions which is difficult to achieve by means of any traditional reinforcement. The test results of compressive strength, splitting tensile strength, and flexural strength for cubes with different percentage of steel fibers are presented in Table 3. Fig. 8 shows the test setup of the three tests.

3.4 Results of tested beam specimens

Fifteen specimens of reinforced concrete beams have been designed to fail in shear and testing under monotonic loading. The first shear crack, cracking patterns, mid-span deflection and ultimate shear load were recorded and the results were discussed. The cracking pattern at failure for the test specimens are shown in Fig. 9. The values of load and deflection for specimens of groups $G1$, $G2$, and $G3$ are given in Table 4.

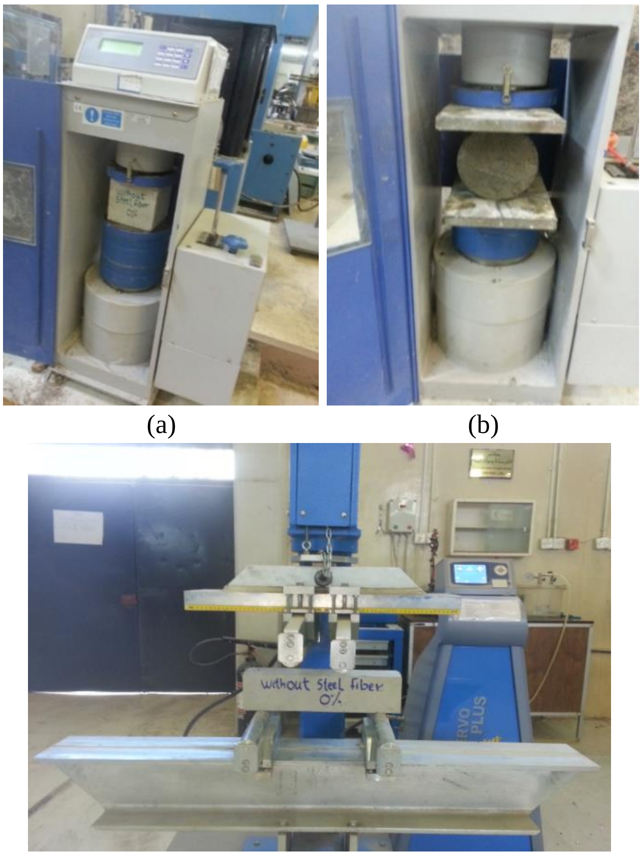

(a) (b)

(c)

Fig. 8 Test setup of concrete specimens: (a) compressive strength test; (b) splitting tensile strength test; (c) flexural strength test

Table 3 Tests results for concrete specimens

Specimen type	Compressive strength (N/mm^2)		Splitting tensile strength (N/mm^2)		Flexural strength (N/mm^2)	
	Value	% increase	Value	% increase	Value	% increase
Reference\ without S.F	33.62	-	2.48	-	4.28	-
With 0.5% S.F	36.08	7.31	3.16	27.40	4.37	2.1
With 0.75% S.F	36.90	9.75	3.33	34.20	4.57	6.7

4. Effect of different parameters on the shear strength

The test parameters considered in this research are steel fibers, shear span to depth ratio (a/d_{min}) and tapering angle (α). The effect of these parameters on the shear strength of non-prismatic beams is discussed below.

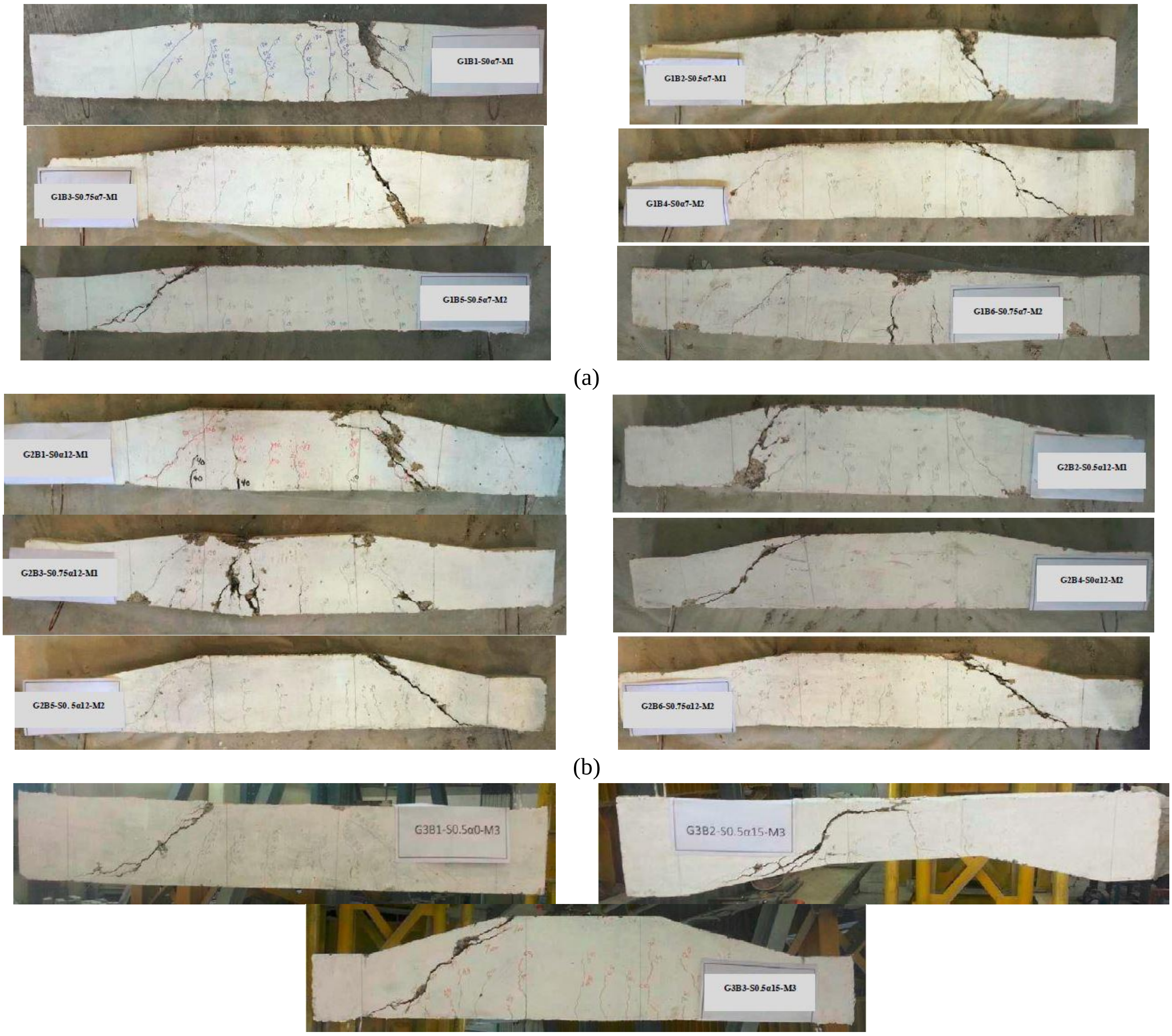

(a) (b) (c)

Fig. 9 Cracking pattern at failure: (a) group *G*1, (b) group *G*2, (c) group *G*3

Table 4 Test results for test specimens

Group	Beam	$a/d_{\min}$	S.F%	Load of the first shear crack (kN)	Mid span def. at first crack (mm)	Ult. load (kN)	Mid span def. at ulti. load (mm)	Increase %		Energy absorption (kN.mm)
								Cracking load	Ult. load	
G1	B1	1.6	0	39.26	3.06	132.99	6.53	-	-	391.22
	B2	1.6	0.50	53.63	3.84	146.29	8.34	38.00	27.71	578.91
	B3	1.6	0.75	65.69	4.62	173.68	11.89	69.04	30.59	1131.31
	B4	2.8	0	33.76	3.85	50.13	6.90	-	-	217.68
	B5	2.8	0.50	40.56	4.35	81.06	8.81	20.00	61.00	373.71
	B6	2.8	0.75	53.99	7.78	101.79	29.98	59.00	103.00	2379.66
G2	B1	1.6	0	37.56	3.14	193.05	12.59	-	-	1106.99
	B2	1.6	0.50	55.36	4.25	212.85	12.07	47.39	10.25	1308.14
	B3	1.6	0.75	69.63	4.04	251.54	22.07	85.38	30.29	4169.96
	B4	2.8	0	34.20	3.81	53.99	5.53	-	-	152.77
	B5	2.8	0.50	44.20	4.13	88.92	8.23	29.23	64.69	413.18
	B6	2.8	0.75	58.99	4.93	93.26	8.13	72.24	72.73	427.22
G3	B1	2.4	0.50	44.26	4.20	84.06	8.53	-	-	407.29
	B2	1.8	0.50	25.29	3.18	42.69	8.48	-	-	426.88
	B3	1.8	0.50	34.06	2.41	102.12	8.11	-	-	479.90

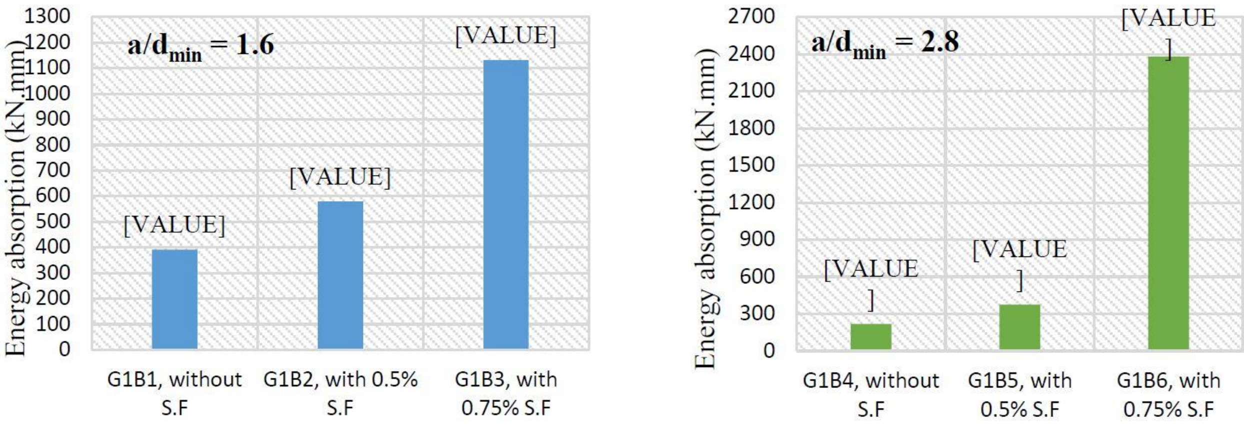

(a)

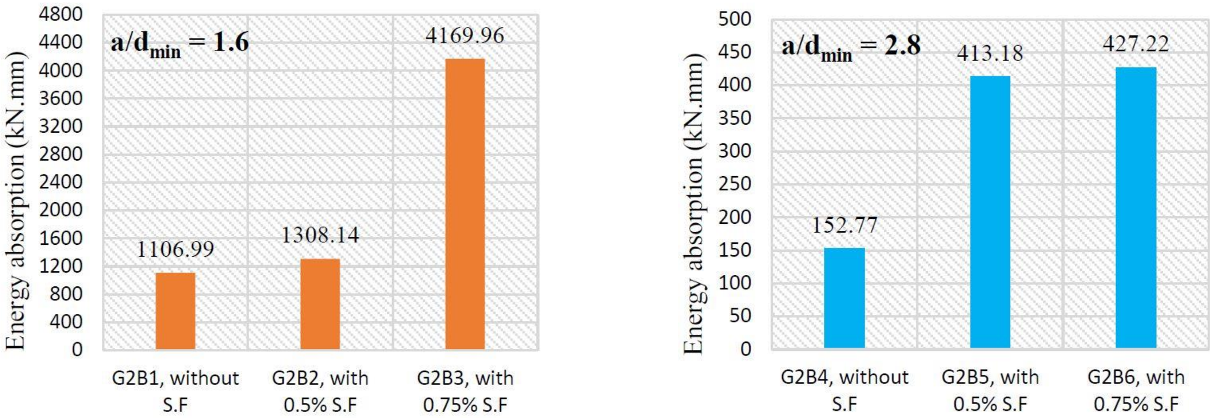

(b)

Fig. 10 Energy absorption capacity: (a) group *G*1, (b): group *G*2

4.1 Steel fibers

Through the results obtained from tested specimens, it was observed that the steel fibers has significantly affected the shear strength of concrete. The presence of steel fibers in concrete enhanced the mechanical properties and energy absorption capacity of concrete through increasing the shear cracking load, ultimate load, the tensile strength and ductility of the test specimen. Steel fibers also decrease the crack width, control of concrete cracking, transfer stresses from the cracks formation in every direction and ability to change failure mode from brittle to ductile failure as a result of the crack-bridging action of the fiber.

Ductility and energy absorption capacity were the main material properties enhanced by using steel fiber. Some of the specimens failed due to flexure such as in beam *G*1*B*6 and *G*2*B*3 with increase the steel fiber percent up to 0.75%. This is related to the fact that the steel fibers play an important role in changing the failure mode from shear to flexural failure. The enhancement of energy absorption by steel fibers and the effect of steel fibers on the shear strength of reinforced concrete beams are illustrated in Figs 10 and 11 respectively.

4.2 Shear span to depth ratio (a/d_{min})

The test results for groups *G*1 and group *G*2 revealed that the shear span to depth ratio (a/d_{min}) had a significant effect on the shear capacity of the test specimens. When the value of shear span to depth ratio (a/d_{min}) was less than (2) the shear capacity of test specimens became higher than that when the shear span to depth ratio value was greater than (2). The reason is relating to the formation of a compression strut and the strut action prevailed and the shear resistance was high for the shear span to depth ratio (a/d_{min}) was less than (2). By this mechanism, the applied load transferred directly to supports through compression struts leading to increasing the capability of the beam to resist more loads. In the second case of shear span to depth ratio with (a/d_{min}) greater than (2), the shear capacity of the beam was reduced due to the formation of beam action. The effect of shear span to depth ratio on the shear strength of test specimens is shown in Fig. 12.

4.3Tapering angle (α)

The effect of tapering angle (α) was clear from the obtained results. When the tapered angle increased, the load of the first shear crack and the ultimate shear capacity were increased. The tapering angle develops an arch mechanism which allows the load to be distributed in terms of several cracks along the inclined length before the main diagonal cracks develop. The effect of tapering angle on shear strength is shown in Fig.13. The load deflection behavior and energy absorption capacity for group G3 are shown in Fig. 14.

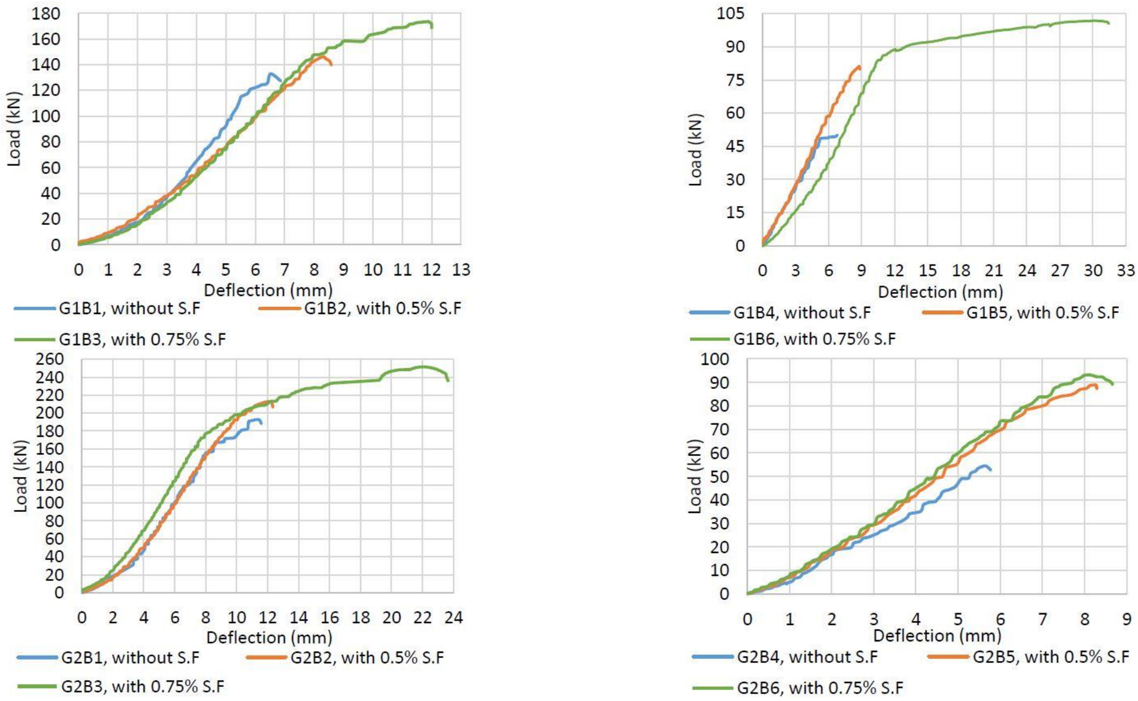

Fig. 11 Effect of steel fibers on shear strength of non-prismatic reinforced concrete beams

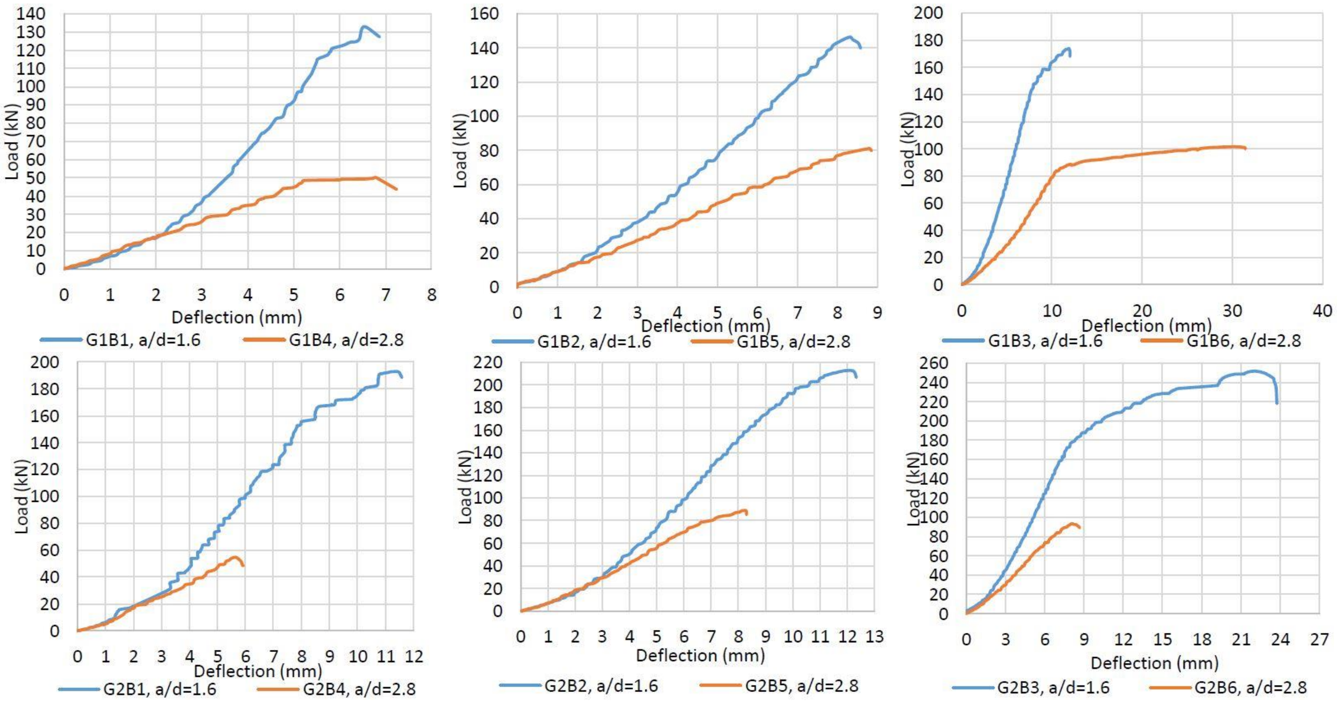

Fig. 12 Effect of shear span to depth ratio of shear strength of test specimens (d=$d_{\min}$)

5. Available empirical equations for shear strength prediction

Debaiky and El-Niema (1982) proposed an equation to predict the cracking shear strength of haunch beam (Vpc) which is based on regression analysis of their experimental results as follow

$$Vpc=(0.16 \times \sqrt{f'c} + 17\,\rho_w\,\frac{V_u\,d_s}{M_u}) \times bd_s(1 + 1.7\tan(\alpha)) \tag{1}$$

Where:

ds = the effective depth of beam at the support sections

ρ_w = the ratio of longitudinal reinforcement

V_u= ultimate applied shear force at the critical section

M_u = ultimate applied moment at the critical section

α=tapering angle

The effective depth at the critical section (d_{cr}) which is measured from the support as follows

$$dcr = ds\,(1 + 1.7\,tan\,\alpha) \tag{2}$$

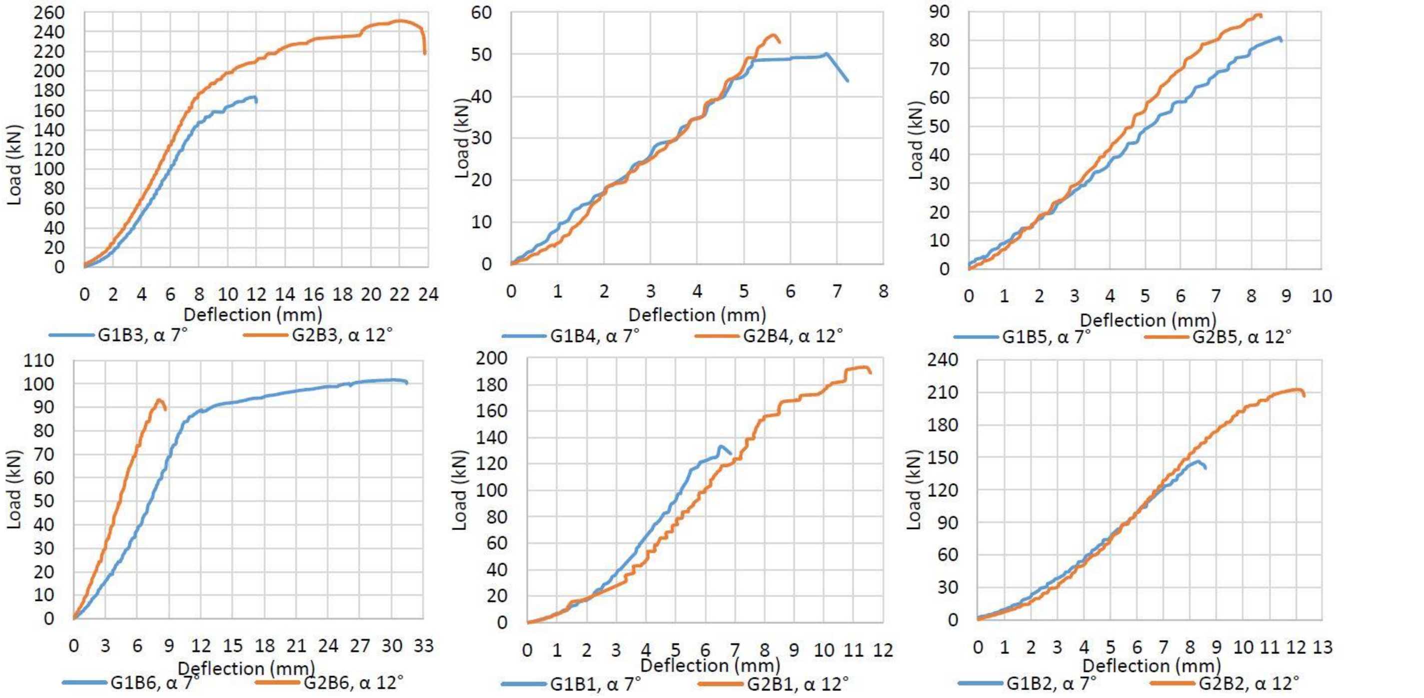

Fig. 13 Effect of tapering angle on shear strength

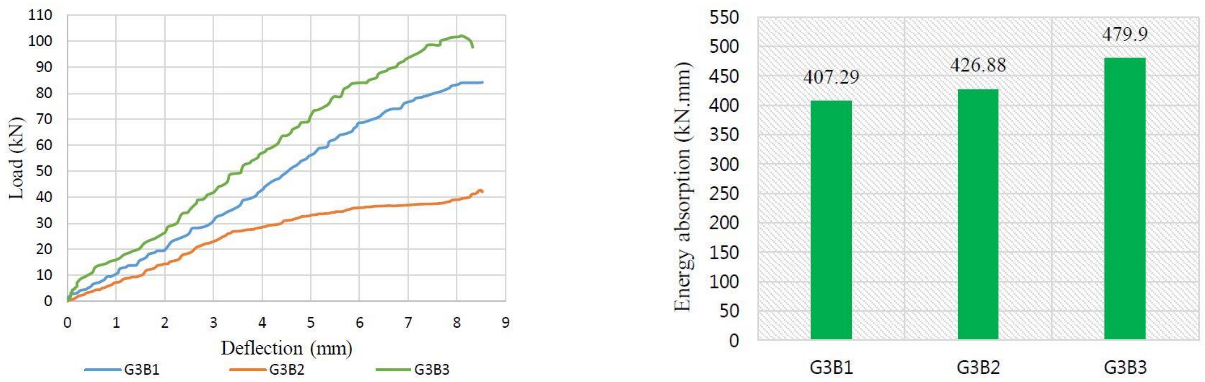

(a) (b)

Fig. 14 (a) The load deflection behavior; (b) energy absorption capacity for group $G3$

Tena-Colunga *et al*. (2008) proposed an empirical equation to predict the cracking shear strength which was based on the results of their experimental program as follows

$$Vpc = (0.16 \times \sqrt{f'c} + 17\,\rho_w \frac{V_u\, d_{cr}}{M_u}) \times bd_{cr} \tag{3}$$

In which all parameters are previously defined but

$$dcr = dmin\,(1 + 1.35\, tan\,\alpha) \leq \left[\left(\frac{\left(h_{max}\, h_{min} - (h_{\max})^2\right)}{2l_h} + h_{max}\right) - r\right] \tag{4}$$

Where $h_{\max}$, $h_{\min}$, are the maximum and minimum total depth of the beam while $d_{\min}$ is the minimum effective depth of the beam. The parameters (l_h) and (r) are the length of the tapered part of the beam and the concrete cover respectively.

Both of the above equations didn't take into account the effect of steel fibers.

6. The proposed equation for cracking shear strength prediction

Based on the obtained experimental results and regression analysis by using MATLAB (R 2010 a), the following equation is proposed with respect to the ACI 318M (2014) by fitting the experimental data using a three dimensional surface as follows

$$V_c = V_{cr} = \left[0.134\sqrt{f'c} + 14.25\rho_w \frac{V_u d_{cr}}{M_u}\right]$$
$$\left[1 + 0.955(S_f) + 0.835\tan(\alpha)\right][bd_{cr}] \tag{5}$$

Where

V_{cr} is the cracking shear strength of concrete (MN);
$f'c$ is the concrete cube strength (MPa);
S_f is the steel-fiber ratio (percent);
b is the width of the beam (m);
d_{cr}, C are the depth at critical section and the horizontal

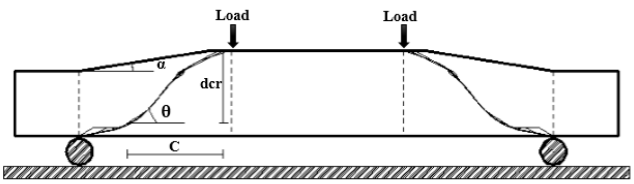

Fig. 15 Idealized shear crack and its inclination angle

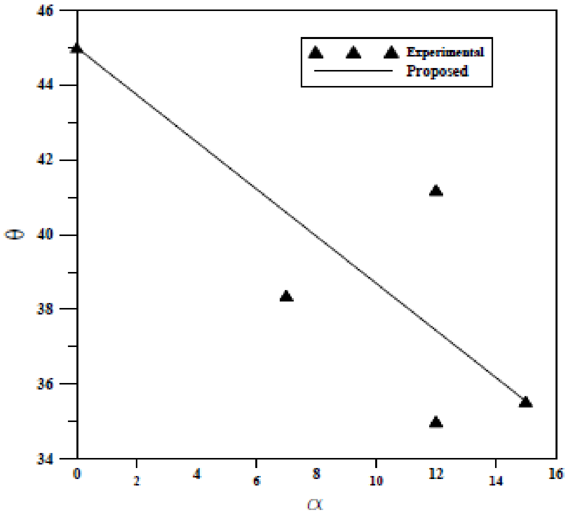

Fig. 16 Crack angle-tapering angle relationship

projection of the main shear crack respectively as shown in Fig. 15 which were previously proposed by MacLeod and Houmsi (1994) as follows(d_{cr} and C are in m)

$$d_{cr} = [d_{min} + C\tan(\alpha)]$$
$$C = d_{min}\frac{(1+\tan(\alpha))}{\tan(\theta)-\tan(\alpha)} \quad (6)$$

In which (θ) is the inclination angle of the main shear crack. Based on the present experimental results, a relationship between (θ) and (α) is shown in Fig. 16 and the following equation is proposed

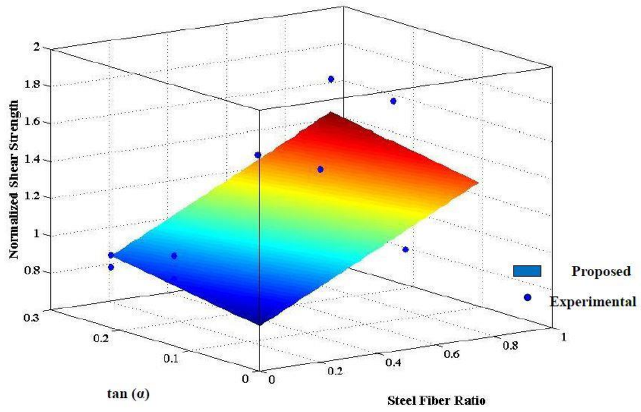

Fig. 17 Variation of normalized cracking shear force with respect to (S_f) and (tan (α))

$$\theta = 45 - 0.63\alpha \quad (7)$$

For practical considerations, the value of d_{cr} is limited such that $(d_{cr} \leq h_{\max} - r)$ .The obtained experimental results are plotted as shown in Fig. 17 which shows the normalized cracking shear strength as a function of (S_f) and tan (α) . The experimental cracking shear force is normalized with respect to the shear strength given by ACI 318M (2014) as follows

Normalized cracking shear strength=

$$\overline{V_{cr}} = \frac{V_{cr}}{\left[0.16\sqrt{f'c} + 17\rho_w\frac{V_u d_{cr}}{M_u}\right]bd_{cr}} \quad (8)$$

The proposed equations are obtained by using Matlab version 7 (R2010a). The results obtained from the proposed Eq. (5) is compared with those obtained from Tena-Colunga *et al.* (2008) and the results obtained by Debaiky and El-Niema (1982) as given in Table 5. It is clear from the presented results that the predicted cracking shear force using the proposed equation is in good agreement with the experimental results in comparison to the available

Table 5 Comparison of the predicted cracking shear with the available empirical formulas for groups (G1) and (G2)

Beam	Vcr Exper. (kN)	Vcr Proposed (kN)	$\frac{Vcr\ Prop.}{Vcr\ Exper.}$	Debaiky and El-Niema		Tena-Colunga *et al.*	
				Vcr (kN)	$\frac{Vcr}{Vcr\ Exper.}$	Vcr kN)	$\frac{Vcr}{Vcr\ Exper.}$
G1B1	19.63	12.71	0.65	15.82	0.81	13.35	0.68
G1B2	26.82	18.80	0.70	16.57	0.62	13.78	0.51
G1B3	32.85	21.86	0.67	16.74	0.51	13.92	0.42
G1B4	16.88	12.71	0.75	13.67	0.81	13.35	0.79
G1B5	20.28	18.80	0.93	14.12	0.70	13.78	0.68
G1B6	27.00	21.86	0.81	14.26	0.53	13.92	0.52
Average	-	-	0.75	-	0.66	-	0.60
G2B1	18.78	16.52	0.88	18.73	1.00	14.32	0.76
G2B2	27.68	23.98	0.87	19.37	0.70	14.80	0.53
G2B3	34.82	27.73	0.80	19.57	0.56	14.95	0.43
G2B4	17.10	16.52	0.97	14.93	0.87	14.32	0.84
G2B5	22.10	23.98	1.09	15.44	0.70	14.80	0.67
G2B6	29.46	27.73	0.94	15.61	0.53	14.95	0.51
Average	-	-	0.92	-	0.73	-	0.62

empirical equations. However, the cracking shear strength of the second group is predicted better than that of the first group. This can be attributed to the mathematical operations of the regression analysis. It can be seen that when the tapering angle of the second group has been changed from (7°) to (12°) and the cracking shear strength was increased slightly. Accordingly, the regression analysis process aims to minimize the estimation error which is related mainly to the second group (due to the change of tapering angle (α)). Hence, the suggested linear 3D surface is closer to the data and gives a better prediction for the behavior of the second group. The square of the regression factor (*R*-square) of the proposed equation for cracking shear strength is (R^2=0.76).

7. Conclusions

Based on the results of the experimental program carried out, the following conclusions can be drawn:

- The mechanical properties of concrete (compressive strength, splitting tensile strength and flexural strength) may be improved or adversely affected by the addition of hooked end steel fibers depending on its content.
- The concrete compressive strength increased with the addition of steel fibers. Specimens reinforced with (0.5% or 0.75%) showed an increase in compressive strength of about (7.31%) and (9.75%) respectively compared to the reference specimen.
- The splitting tensile strength increased with the increase in steel fiber content. The increase in splitting tensile strength in specimens reinforced with (0.5% or 0.75%) was (27.40%), (34.20%) respectively compared to the reference specimen.
- Concrete prisms reinforced with (0.5%) or (0.75%) of steel fiber showed an increase in flexural strength of about (2.1%) and (6.7%) respectively compared to the reference specimen.
- The experimental results indicated that the steel fibers increase significantly the shear strength of concrete. The increase is directly proportional to the percent of steel fiber content. The maximum increase in ultimate shear strength was (103%) for specimens with steel fiber content (0.75%) by volume of concrete.
- The addition of steel fibers also caused a decrease in shear crack width, increased the ductility of the beam. The mode of failure had been changed from brittle failure to ductile. Also, the addition of steel fibers caused an increase in energy absorption of the beam. This increase depending on the percent of steel fibers. It was found that the maximum increase in energy absorption capacity was (993.18%) for a steel fiber ratio of (0.75%) by volume of concrete.
- The ultimate shear strength was inversely proportional to shear span to depth ratio ($a/d_{\min}$), for all test specimens. When the ($a/d_{\min}$) ratio increased from (1.6) to (2.8) the ultimate shear strength had an average decrease of (56.90%).
- The addition of steel fiber to concrete reduced the workability of the concrete mixture. The obtained reduction of the slump was in the range of (50 to 70) mm. The decrease in workability depending on the amount of steel fiber content.
- The tapering angle had an obvious effect on the shear strength of concrete. It was found the maximum increase in load carrying capacity was (45.49%).
- The predicted cracking shear from the proposed equation is in good agreement with the experimental results with an overall ($\frac{Vcr\ prop.}{Vcr\ exper.}$) average of (0.84).

Acknowledgments

The authors wish to thank the staff of the Civil Engineering Laboratory of Al-Nahrain University for their support during the experimental part of this work.

References

ACI 318M (2014), Building Code Requirements for Structural Concrete and Commentary, American Concrete Institute, Farmington Hills, MI, USA

Alejandro, P.C., Patricio, P., Aurelio, M. and Miguel, F.R. (2012), "Effect of load distribution and variable depth on shear resistance of slender beams without stirrups", *ACI Struct. J.*, **109**(109), 595-603.

ASCE- ACI Task Committee 426 (1973), "The shear strength of reinforced concrete member", *J. Struct. Div*.

ASTM C 78 (2002) *Standard Test Method for Flexural Strength of Concrete (Using Simple Beam with Third-Point Loading)*, Annual Book of ASTM Standards, American Society for Testing and Materials.

ASTM C496/C496M (2004), Standard Test Method for Splitting Tensile Strength of Cylindrical Concrete Specimens, ASTM International, West Conshohocken, PA.

B.S. 1881, Part 116 (1989), Method for Determination of Compressive Strength of Concrete Cubes, British Standards Institution.

Babar, T.V., Joshi, K.P. and Shinde, N.D. (2015), "Shear strength of steel fiber reinforced concrete beam without stirrups", *Int. J. Adv. Eng. Technol.*, **6**(2), 15-18.

Chenwei, H., Koji, M. and Junichiro, N. (2015), "Shear resistance mechanism of reinforced concrete haunched beams without shear reinforcement", *J. JSCE*, **3**, 230-245.

Daniel de Lima, A., Fernanda, G.T.N., Romildo, D.T.F. and Moacir, A.S. (2014), "Shear strength of steel fiber-reinforced concrete beams", *Acta Scientiarum. Technol.*, **36**(3), 389-397.

Debaiky, S.Y. and El-Niema, E.I. (1982), "Behavior and strength of reinforced concrete haunched beams in shear", *ACI Struct. J.*, **79**(3), 94-184.

Hai, H.D. (2009), "Shear behavior of steel fiber reinforced concrete beams without stirrups reinforced", Ph.D. Thesis, University of Michigan, Michigan.

James, I.D., Vellore, S.G. and Melvyn, A.G. (2002), "State-of-the-art report on fiber reinforced concrete", ACI Committee 544.

Keskin, R.S.O. (2017), "Predicting shear strength of SFRC slender beams without stirrups using an ANN model", *Struct. Eng. Mech.*, **61**(5), 605-615.

MacLeod, I.A. and Houmsi, A. (1994), "Shear strength of haunched beams without shear reinforcement", *ACI Struct. J.*, **91**(1), 79-89.

Mahadik, A.S., Kamane, K.S. and. Lande, C.A. (2014), "Effect of steel ribers on compressive and flexural strength of concrete", *Int. J. Adv. Struct. Geotech. Eng.*, **3**(4), 388-392.

Mohammed, S.A. (2014), "Diagonal cracking capacity and ultimate shear strength of slender RC beams without web

reinforcement", *Jordan J. Civil Eng.*, **8**(1), 97-112.
Sasturkar, J.P. (2012), "High performance and serviceability of fibre reinforced concrete", *WIT Tran. Built Environ.*, **124**, 299-307.
Sika ViscoCrete -5930 (2010), Product Data Sheet, Edition 6, Version no. 01.10.
Sudheer, R.L., Ramana, R.N.V. and Gunneswara, R.T.D. (2010), "Shear resistance of high strength concrete beams without shear reinforcement", *Int. J. Civil Struct. Eng.*, **1**(1), 101-113.
Tena-Colunga, A., Archundia-Aranda, H.I. and González-Cuevas, Ó.M. (2008) "Behavior of reinforced concrete haunched beams subjected to static shear loading", *Eng. Struct.*, **30**(2), 478-492
Vu Hong, N. (2011), "Shear design of straight and haunched concrete beams without stirrups", Ph.D., Technical University of Hamburg, Hamgurg.

CC